

Interplanetary Proton Fluence Model: JPL 1991

J. FEYNMAN, G. SPITALE, AND J. WANG

Jet Propulsion Laboratory, California Institute of Technology, Pasadena

S. GABRIEL

Department of Astronautics and Aeronautics, University of Southampton, Southampton, England

We describe an updated predictive engineering model for the interplanetary **fluence** of protons with energies >1 , >4 , >10 , >30 , and >60 MeV. This has been the first opportunity to derive a model from a data set that has been **collected** in space over a long enough period of time to produce a valid sample of solar proton events. The model provides a quantitative basis for estimating the exposures to solar protons of spacecraft during missions of varying **length** and of surfaces and atmospheres of solar system objects. It is derived from the set of data collected by the IMP and OOO spacecraft between 1963 and 1991. The >10 and >30 MeV data sets cover the period from 1963 to day 126 of 1991. The >1 , >4 , and >60 MeV data sets were collected between 1973 and 1991. Both data **sets** contain several major proton events (>1 0-MeV **fluences** exceeding 3 or 4×10^9 protons/cm²) comparable to the 1972 event. The method of statistical analysis used in producing the model of the proton environment is the same as that used for earlier models. For the **cases** of the >10 and >30 MeV particles, the **fluences** are somewhat lower than in our earlier model (JPL 85). No >1 , >4 , and >60 MeV proton **fluence** models have been published in the literature previously. We present our results in a convenient graphical form which may be used to calculate the 1 AU **fluence expected** at a given confidence level as a function of the length of the exposure. A method of extending this estimate to other heliocentric distances is described.

INTRODUCTION

This study was carried out to increase the accuracy and energy range of predictive models of interplanetary proton **fluences**. Such an estimate is often **needed** when spacecraft spend a significant amount of time in the interplanetary environment. The model described here provides a quantitative basis for estimating the exposures of spacecraft during missions of varying length and of surfaces and atmospheres of solar system objects to solar protons. Coupled with longer-term models of solar activity, it will be of help in considering the effects of solar protons on solar system objects over longer time scales. The interplanetary proton **fluence** below about 100 MeV is dominated by solar protons. Total **fluence** during an exposure is due to the combined effect of the discrete solar events that produce high-energy protons during that exposure. The distribution of sizes of the proton events is such that the total **fluence predicted** for a spacecraft mission will be due, in the main, to a small number of very high **fluence** events [King, 1974; Feynman *et al.*, 1990a, b] if any such events take place. It is therefore very important to correctly estimate the probability of **occurrence** of large events. These major events are quite rare, and many years may pass between major events. As a result, data must be collected for decades before a valid sample of possible proton events can be detected. The new model described here is the first model that has been able to use a data set collected by a single set of experiments over such a long period of time that the population of major events is probably well sampled.

The model presented here is intended to replace our earlier model (JPL 1985) that used proton data collected up until 1985 [Feynman *et al.*, 1990a]. This earlier model is now in the National Space Science Data Center (NSSDC) data base and is

currently in widespread use. That model was a revision of the earlier King [1974] model, which used data from only one solar Cycle.

The occurrence frequency of the major events that dominate the total fluence do not appear to be randomly distributed in time. Instead, they appear to be much more common in some solar cycles than in others. In particular, in the 25 years between 1963 and 1988 there was only one major event (1972). In contrast, 3 or 4 major events occurred in the short time period from 1957 to 1963, and 4 or 5 major events have occurred during the last few years (1989 to 1991). It is therefore essential that the data set used is collected over several solar cycles so that it contains a good statistical sample of the major events. At the time the JPL 1985 model was constructed, only one major proton event had taken place since 1963 when data collection in space had become routine. In the JPL 1985 model this problem was dealt with by using data that had been collected before 1963. Although those data were of surprisingly good quality (see Feynman et al. [1990b] for a discussion), they were collected and analyzed with different techniques from the post-1963 data. For that reason the data set used in the JPL 85 model did not form a uniform data set. The occurrence of major proton events in the last 2 or 3 years gives us the opportunity to correct that weakness in the JPL 1985 model. At the same time we are now able to extend the model energy range.

DATA BASE

From 1963 to the present, instruments have been observing proton fluxes in space using a series of closely related instruments on the IMP 1, 2, and 3, SOGO 1 and IMP 5, 6, 7, and 8 series of spacecraft. Armstrong et al. [1983] collected the data available at that time and edited it for valid solar particle responses. The data set used in this study is an extension of that data set and consists of a nearly time continuous record of daily average fluxes above the energy thresholds of 1, 4, 10, 30, and 60 MeV. The time periods used cover from day 331 of 1963 through day 126 of 1991 for the >10, >30 and >60 MeV data. The >1 and >4 MeV data begin on day 270 of 1972 and hence do not include the famous August 1972 event. These lower-energy data sets also end on day 126 of 1991.

Individual proton events are associated with individual coronal mass ejections [Kahler, 1987]. However, it is well known that strong coronal mass ejections (CME) and major proton events typically occur in series associated with single active centers as the center is carried across the face of the Sun by the solar rotation [Malitson and Webber, 1962]. If, in a model designed to estimate the expected proton fluence for engineering purposes, each individual CME-proton event is assumed to be independent in time from every other CME-proton event the statistical properties of the distribution of high-fluence events will be different from the actually occurring distribution. To take account of this problem, the proton events considered in our models are defined as the total fluence occurring over series of days during which the proton fluence exceeded a selected threshold. The threshold is selected separately for each energy range and is listed in Table 1. This

[Table 1]

procedure is the same as that used in our earlier models [Feynman et al., 1990a, b].

Using the event fluences determined in this way, we studied the distribution of sizes of the event integrated fluences in our data set. In our earlier studies [Feynman et al., 1990a, b] we showed that the sunspot cycle was divided into two periods: a **high-fluence**, active Sun period of 7 years and a **low-fluence** quiet Sun period of 4 years. The active period began 2 years before the year of solar maximum and included the fourth year after solar maximum. Our approach differed from that of earlier workers in that we used years defined relative to solar maximum determined to 0.1 years. This definition resulted in a much **clearer bimodal** solar cycle variation than that found in earlier studies. Figure 1 shows an update of those results, and Figures 2a and 2b present a more detailed characterization of the **bimodal** nature of solar cycle variation.

Since the **bimodal** character of the results continues, it is useful to consider the statistical properties of the events occurring during the active period separately from those occurring during the quiet periods. Because the quiet periods are so quiet, we can assume that no significant proton fluence exists during those periods and that the only model needed is that for the active periods. In this study we use data collected during the 7 active years of the cycles only. Sunspot maximum for the current cycle occurred at 1989.9 rather than at 1990.9 as would be expected based on an 11-year cycle. For studies of the effects of solar protons on astronomical bodies, the fluence for 1 1-year solar cycles should be taken as equal to the fluence for 7 active years.

STATISTICAL CONSIDERATIONS

In Figures 3a through 3e we compare the distribution of event integrated fluences to lognormal distributions. The events have been ordered according to the log of the fluence and plotted versus the percent of observed events that have a magnitude less than the given event. To be more exact, fluences were plotted against $(i * 100) / (n + 1)$, where i is the rank of the events used in the data set and n is the number of events in the data set. The horizontal axis of the plot is scaled, so that a data set that is distributed lognormally will appear as a straight line. Now the real distribution of the data is not lognormal since in the real data there are always more events the smaller the size of the event [Feynman, 1990a], whereas for a lognormal distribution there is a mean event size and the number of events decreases for events both smaller and larger than that mean. For this reason (and other less important reasons [see Yucker, 1972; Feynman et al., 1990a, b]) the distributions cannot be expected to be fit by a straight line for fluences less than the average of the data set. However, the estimate of the total fluence accumulated during a mission is dominated by the estimate of the probability of occurrence for large events and will not be changed due to the underestimate of the probability of occurrence of the small events. The important question is the estimate of occurrence of the largest events. In earlier studies and in this study we studied the effect of using other fitting functions such as type H and type III extreme value functions (see King [1981] for a discussion of extreme value functions) and kappa functions but the fits to the

Figure 1
Figs. 2a, 2b

Figs. 3a, 3b, 3c, 3d, 3e

data were not improved. A polynomial was also fit to the data, and the possibility of using that function was investigated. However, for a polynomial fit there is always a largest event predicted for the function (i.e., an event fluence for which the probability of exceeding that fluence is zero). This is probably not true for the real distribution. However, more important for a predictive model is the fact that the size of that maximum event depended strongly on the order of the polynomial used and the expected fluence for a mission depended strongly on the size of that maximum event. Under these circumstances it seemed best to continue to use the traditional method of fitting the data with a lognormal fit which is chosen to fit the high end of the fluence data. There remains a certain amount of individual judgement in choosing that fitted curve. We have chosen fits which appeared to be reasonably conservative. The data and the fits are given in Figures 3a through 3e. The parameters of the fits have no physical meaning as can easily be seen by noting that the mean of the distribution will change if a lower cutoff is chosen for the plot. (This of course would not be true if the data were really distributed in a lognormal fashion.) If a different lower cutoff is chosen, the fluence predicted for a mission would not change, of course, because the mean, standard deviation, and number of events per year would also all change. The changes in the mean, standard distribution, and number of events per year would be such that the total fluence estimates would remain unchanged. The parameters of the fits actually used are given in Table 2.

The parameters describing the fits in Figures 3a through 3e were used in a Monte Carlo simulation as described by Feynman *et al.* [1990a]. The details of that calculation are described in Appendix A for completeness. A list of the fluences for the 10 largest events in each energy range is given in Tables 3a through 3e.

RESULTS AND USE OF THE MODEL

The purpose of the simulation described here is to generate a curve giving the probability of exceeding a given fluence during a mission or exposure of a selected duration. The results for a selection of mission lengths are shown in Figures 4a through 4e. These figures give the probability of exceeding a given fluence during the life of the mission assuming a constant heliocentric distance of 1 AU. Five mission lengths are shown in each figure. In calculating mission length (or, more generally, exposure time) only the time the spacecraft or solar system body spends in interplanetary space during the solar cycle active years should be included.

To use Figures 4a through 4e to estimate mission fluences, find the line that corresponds to the desired mission length. For exposure duration large compared to a solar cycle, the fluence in a single 11-year cycle should be assumed to be equal to "7-year" fluence. Locate the "confidence" level required, recalling that a confidence level of say 95% means that only 5% of missions identical to the one considered will have fluences larger than that determined for the 95% confidence level (i.e., probability + confidence level = 100%). Then the abscissa gives the fluence that will not be exceeded with the selected confidence level.

Figure 3

Figure 3

The ... of ...

(Figs. 4a, 4b, 4c, 4d, 4e)

In Table 4 we give our new fluences for two confidence levels for a 2-year mission, and when appropriate, we compare them with the values derived from the JPL 85 model.

A comparison of the JPL 85 results with the JPL 91 results shows that the new model predicts a somewhat milder environment at >10 and >30 MeV but that the fluence is declining less steeply with energy threshold. We believe that this model, based as it is on a 28-year-long uniform data set, is more reliable than our earlier model.

To find the fluence for a mission in which the vehicle or solar system body does not remain at 1 AU, the fluence at 1 AU should be multiplied by a factor which depends on the actual trajectory, i.e., the integration of the radial dependence of the fluence over the trajectory. In the work by Feynman et al. [1990], we suggested using the radial dependence recommended by the working group on solar particle events of a workshop on Interplanetary Charged Particle Environment held at the Jet Propulsion Laboratory, Pasadena, California, in March 1987 [Feynman et al., 1988]. For spacecraft missions they recommended using an inverse cube dependence for $R < 1$ AU and an inverse square dependence for $R > 1$ AU. These radial dependencies are worst case choices but were the best estimates that could be made using the data then available. No further work on this problem has been reported in the literature, and so these recommendations must remain in place. Here, for solar system bodies, we suggest using an inverse square dependence for both $r > 1$ AU and $r < 1$ AU because a "most probable" estimate is required for this problem rather than a "worst case" estimate.

Note that in the models discussed here the fluence is a steep function of the confidence level. In some applications a small lowering of the confidence level requirement may be acceptable and result in a large enough decrease in estimated fluence to eliminate an otherwise important problem. For long-term solar system body exposure estimates, the total fluence will be given by

$$\int F(p)f(p) dp$$

where $F(p)$ is fluence for a single solar cycle at a given probability level and $f(p)$ is the probability distribution function.

DAILY FLUENCES

For some spacecraft engineering applications the important parameter is the daily average flux rather than the mission integrated fluence. The distribution of daily fluence has been generated for each of the energy ranges separately and is shown in Figures 5a through 5e. Each of the distributions has been fit with a straight line that passes through the data in the 80 percentile range. However, as the energy increases an unmistakable deficit of large fluence days develops. The cause of this effect is not known. It may be a real effect in the phenomena or an effect of averaging over a clock day rather than over worst case 24-hour data. We fitted the highest fluence data with a separate straight line to demonstrate this effect. A rough estimate of the number of days during which the fluence can be expected to exceed a given value can be made from the graphs and the number of events in each graph (Table

Table 4

Fig 5a, 5b, 5c, 5d, 5e

2) and the number of years during which the data were collected (Table 2). The ten highest fluence days for all energy ranges are given in Tables 5a through 5e.

1 Table 5a, 5b, 5c, 5d, 5e

CONCLUSIONS

We now have proton fluence data from more than three solar cycles. These data have been used to derive three interplanetary fluence models [King, 1974; Feynman et al., 1990a; and the present paper]. The >10 and >30 MeV fluences predicted by these models differ by factors of approximately 2. This stability in the models reflects the stability in the distribution derived from the data sets each of which used data confined to a limited period of time. The current model uses the most uniform and extensive data set and is considerably more reliable than the earlier models. In addition, it extends the energy range so that the present range is from >1 to >60 MeV. We recommend this model for use by engineers dealing with design problems involving single-event effects, total dose and dose rate effects, and solar panel degradation. The model may also be used to estimate exposures of surfaces and atmospheres of solar system objects to solar protons.

APPENDIX A: STATISTICAL ANALYSIS OF SOLAR EVENT DATA

The cumulative probability distribution of the high fluence portion of the data can be fit quite well with a lognormal distribution (i.e., a straight line in Figures 3 and 5). Let f_p be the proton fluence associated with a particular event: f_p can be written as $f_p = 10^F$. If f_p is distributed lognormally, then F is distributed normally, and its density function is commonly expressed as

$$f(F) = \frac{1}{\sqrt{2\pi}\sigma} \exp\left[-\frac{(F-\mu)^2}{2\sigma^2}\right] \quad (A1)$$

where σ is the standard deviation of the log distribution and μ is the mean log fluence. The values of these parameters are obtained from the straight line fit to the data. The probability that, during a mission of length t , the total mission fluence will exceed f_p is

$$P(>F, \tau) = \sum_{n=1}^{\infty} p(n, w\tau) Q(F, n) \quad (A2)$$

where $p(n, w\tau)$ is the probability of n event(s) occurring during a mission of length τ if an average of w events occurred per year during the observation period. This probability is assumed to follow a Poisson distribution given by

$$p(n, w\tau) = e^{-w\tau} \frac{(w\tau)^n}{n!} \quad (A3)$$

$Q(F, n)$ is the probability that the sum of all fluences due to n events will exceed 10^F . $Q(F, 1)$ is the probability that the fluence given by that one event which occurred is greater than or equal to 10^F . $Q(F, 2)$ is the probability that the two events occurring had the sum of their fluences greater than or equal to 10^F . $Q(F, 3)$ etc...

The values of the $Q(F,n)$ were derived by simulation using a Monte Carlo method. The Monte Carlo program utilized two subroutines [see Press, 1986]. One is a random number generator, which provides numbers with a uniform distribution on the interval [0,1]. The other applies the Box-Muller method of inverse transformation to obtain a Gaussian distribution of random numbers.

The distribution of random numbers is assumed to be the inverse of a cumulative probability distribution given by

$$P(F) = \int_{-\infty}^F \frac{1}{\sqrt{2\pi\sigma^2}} \exp(-(F-\mu)^2/2\sigma^2) dF \quad (A4)$$

which can be written

$$p(F) = \int_{-\infty}^F \frac{1}{\sqrt{2\pi}} \exp(-t^2/2) dt \quad (A5)$$

where $t = (F-\mu)/\sigma$.

As explained above, the values of μ and σ are obtained from the straight line fit to the data. The largest events are given greater weight than small fluence events in determining the best straight line fit.

Acknowledgments. We thank one of the referees for pointing out the importance of these model for solar system body exposure estimates. The solar particle data relies on observations of the IMP satellite series. The majority of this information derives from the Johns Hopkins University/Applied Physics Laboratory Charged Particle Measurement Experiment on IMP-8. We thank T. P. Armstrong for providing the data set and for many related discussions. The research described in this paper was carried out by the Jet Propulsion Laboratory, California Institute of Technology, under a contract with the National Aeronautics and Space Administration.

The Editor thanks T. P. Armstrong and S. Kahler for their assistance in evaluating this paper.

REFERENCES

- Armstrong, T. P., C. Brungardt, and J. E. Meyer, *Satellite Observations of Interplanetary and Polar Cap Solar Particle Fluxes From 1963 to the Present, Weather and Climate Responses to Solar Variations*, edited by B. M. McCormac, Colorado University Press, Boulder, 1983.
- Feynman, J., T. P. Armstrong, L. Dao-Gibner, and S. M. Silverman, A new interplanetary proton fluence model, *J. Spacecr. Rockets*, 27, 403, 1990a.
- Feynman, J., T. P. Armstrong, L. Dao-Gibner, and S. M. Silverman, Solar proton events during solar cycles 19, 20, and 21, *SOL Phys.*, 126, 385, 1990b.
- Feynman, J., and S. B. Gabriel (Ed.), *Interplanetary Particles in the Environment: Proceedings of a Conference*, Publ. 88-28, Jet Propulsion Laboratory, California Institute of Technology, Pasadena, 1988.
- Kahler, S., Coronal mass ejections, *Rev. Geophys.*, 25, 663, 1987.
- King, J. H., Solar proton fluences for 1977-1983 space missions, *J. Spacecr. Rockets*, 11, 401, 1974.
- King, J. R., *Probability Charts for Decision Making*, second printing, James R. King, Tamworth, NH, 1981.
- Malitson, J. I., and W. R. Webber, A summary of cosmic ray events, in *Solar Proton Manual*, edited by F. B. McDonald, NASA Goddard Space Flight Center, Greenbelt, Md., 1962.
- Press, W. J., B. P. Flannery, S. A. Teukolsky, and S. A. Vetterling, *Numerical Recipes*, p. 192, Cambridge University Press, New York, 1986.

Yucker, W. R., Solar cosmic ray hazard to interplanetary and Earth-orbital space travel, in Proceedings of the National Symposium on Natural and Manmade Radiation in Space, edited by **E. A. Warman**, *NASA Tech. Mere.*, **TM-2440**, 1972.

J. Feynman, **G. Spitale**, and **J. Wang**, Jet Propulsion Laboratory, California Institute of Technology, 4800 Oak Grove Drive, Pasadena, CA 91109.

S. Gabriel, Department of Astronautics and Aeronautics, University of Southampton, Southampton **S095NH** England, U.K.

(Received April 23, 1992;
revised November 2, 1992;
accepted November 3, 1992.)

Copyright 1993 by the American Geophysical Union.

Paper number 92JA02670.
0148-0227/93/92JA-02670\$ 05.00

Fig. 1. Yearly event fluences for protons of energy >30 MeV versus year relative to sunspot maximum.

Fig. 2a. Daily fluence of >10 MeV protons versus time of occurrence for events exceeding 10^7 cm $^{-2}$ over three solar cycles.

Fig. 2b. Daily fluence of >30 MeV protons versus time of occurrence for events exceeding 10^7 cm $^{-2}$ over three solar cycles.

Fig. 3a. Distribution of solar event fluences for solar active years between 1973 and 1991 for protons of energy >1 MeV for which daily averaged flux exceeds 460 cm $^{-2}$ s $^{-1}$ sr $^{-1}$. Straight line is the selected lognormal distribution.

Fig. 3b. Distribution of solar event fluences for solar active years between 1973 and 1991 for protons of energy >4 MeV for which daily averaged flux exceeds 9.2 cm $^{-2}$ s $^{-1}$ sr $^{-1}$. Straight line is the selected lognormal distribution.

Fig. 3c. Distribution of solar event fluences for solar active years between 1963 and 1991 for protons of energy >10 MeV for which daily averaged flux exceeds 9.2 cm $^{-2}$ s $^{-1}$ sr $^{-1}$. Straight line is the selected lognormal distribution.

Fig. 3d. Distribution of solar event fluences for solar active years between 1963 and 1991 for protons of energy >30 MeV for which daily averaged flux exceeds 1.0 cm $^{-2}$ S $^{-1}$ sr $^{-1}$. Straight line is the selected lognormal distribution.

Fig. 3e. Distribution of solar event fluences for solar active years between 1963 and 1991 for protons of energy >60 MeV for which daily averaged flux exceeds 1.0 cm $^{-2}$ S $^{-1}$ sr $^{-1}$. Straight line is the selected lognormal distribution.

Fig. 4a. Fluence probability curves for protons of energy greater than 1 MeV for various exposure times.

Fig. 4b. Fluence probability curves for protons of energy greater than 4 MeV for various exposure times.

Fig. 4c. Fluence probability curves for protons of energy greater than 10 MeV for various exposure times.

Fig. 4d. Fluence probability curves for protons of energy greater than 30 MeV for various exposure times.

Fig. 4e. Fluence probability curves for protons of energy greater than 60 MeV for various exposure times.

Fig. 5a. Distribution of daily proton fluences for solar active years between 1973 and 1991 for protons of energy >1 MeV.

Fig. 5b. Distribution of daily proton fluences for solar active years between 1973 and 1991 for protons of energy >4 MeV.

Fig. 5c. Distribution of daily proton fluences for solar active years between 1963 and 1991 for protons of energy >10 MeV.

Fig. 5d. Distribution of daily proton fluences for solar active years between 1963 and 1991 for protons of energy >30 MeV.

Fig. 5e. Distribution of daily proton fluences for solar active years between 1963 and 1991 for protons of energy >60 MeV.

Fig. 1. Yearly event fluences for protons of energy >30 MeV versus year relative to sunspot maximum.

Fig. 2a. Daily fluence of >10 MeV protons versus time of occurrence for events exceeding 10^7 cm $^{-2}$ over three solar cycles.

Fig. 2b. Daily fluence of >30 MeV protons versus time of occurrence for events exceeding 10^7 cm $^{-2}$ over three solar cycles.

Fig. 3a. Distribution of solar event fluences for solar active years between 1973 and 1991 for protons of energy >1 MeV for which daily averaged flux exceeds $460 \text{ cm}^{-2} \text{ s}^{-1} \text{ sr}^{-1}$. Straight line is the selected lognormal distribution.

Fig. 3b. Distribution of solar event fluences for solar active years between 1973 and 1991 for protons of energy >4 MeV for which daily averaged flux exceeds $9.2 \text{ cm}^{-2} \text{ s}^{-1} \text{ sr}^{-1}$. Straight line is the selected lognormal distribution.

Fig. 3c. Distribution of solar event fluences for solar active years between 1963 and 1991 for protons of energy >10 MeV for which daily averaged flux exceeds $9.2 \text{ cm}^{-2} \text{ s}^{-1} \text{ sr}^{-1}$. Straight line is the selected lognormal distribution.

Fig. 3d. Distribution of solar event fluences for solar active years between 1963 and 1991 for protons of energy >30 MeV for which daily averaged flux exceeds $1.0 \text{ cm}^{-2} \text{ s}^{-1} \text{ sr}^{-1}$. Straight line is the selected lognormal distribution.

Fig. 3e. Distribution of solar event fluences for solar active years between 1963 and 1991 for protons of energy >60 MeV for which daily averaged flux exceeds $1.0 \text{ cm}^{-2} \text{ s}^{-1} \text{ sr}^{-1}$. Straight line is the selected lognormal distribution.

Fig. 4a. Fluence probability curves for protons of energy greater than 1 MeV for various exposure times.

Fig. 4b. Fluence probability curves for protons of energy greater than 4 MeV for various exposure times.

Fig. 4c. Fluence probability curves for protons of energy greater than 10 MeV for various exposure times.

Fig. 4d. Fluence probability curves for protons of energy greater than 30 MeV for various exposure times.

Fig. 4e. Fluence probability curves for protons of energy greater than 60 MeV for various exposure times.

Fig. 5a. Distribution of daily proton fluences for solar active years between 1973 and 1991 for protons of energy >1 MeV.

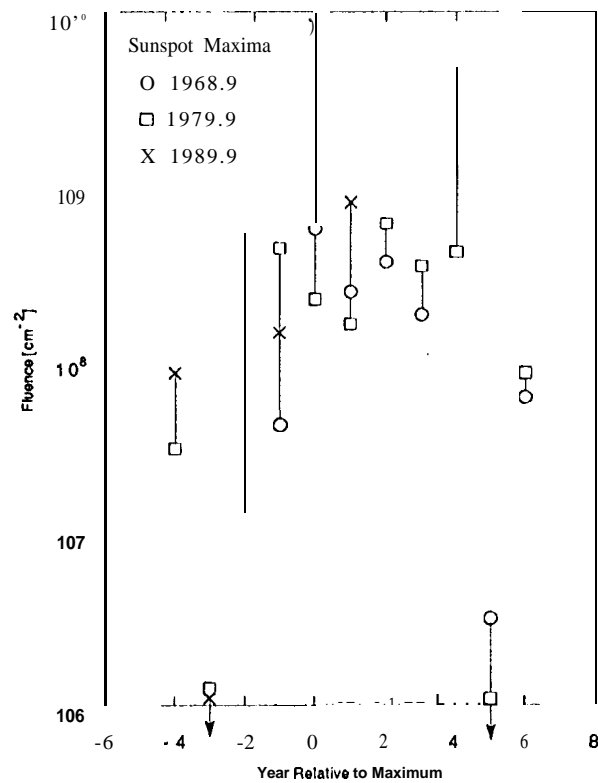
Fig. 5b. Distribution of daily proton fluences for solar active years between 1973 and 1991 for protons of energy >4 MeV.

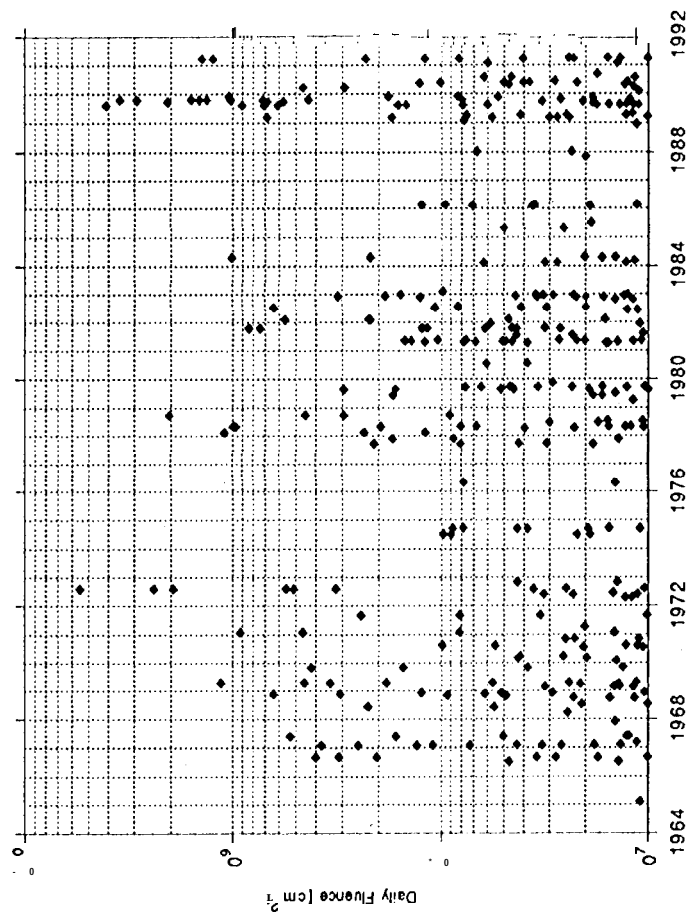
Fig. 5c. Distribution of daily proton fluences for solar active years between 1963 and 1991 for protons of energy >10 MeV.

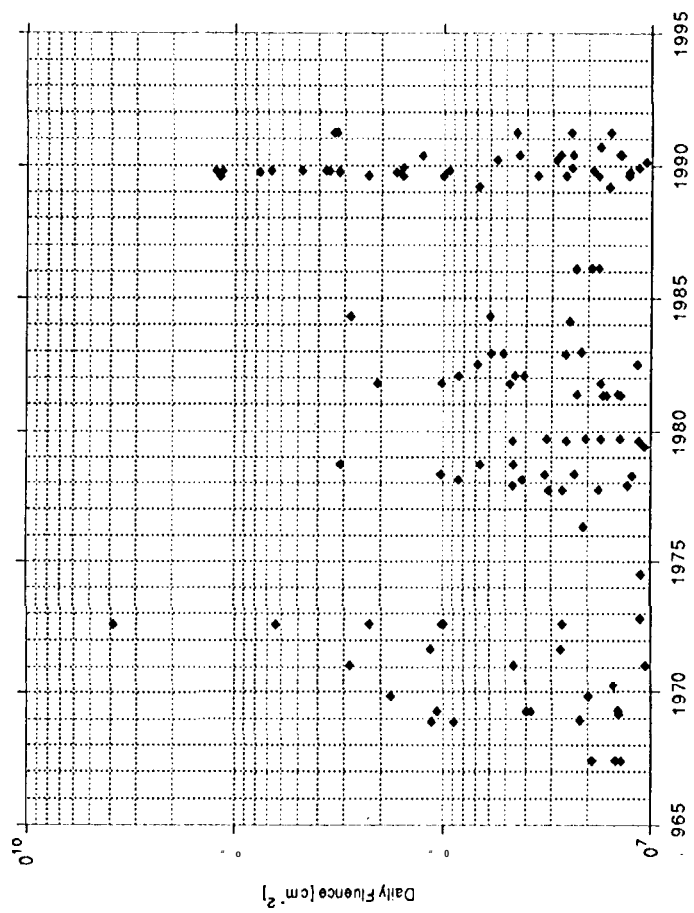
Fig. 5d. Distribution of daily proton fluences for solar active years between 1963 and 1991 for protons of energy >30 MeV.

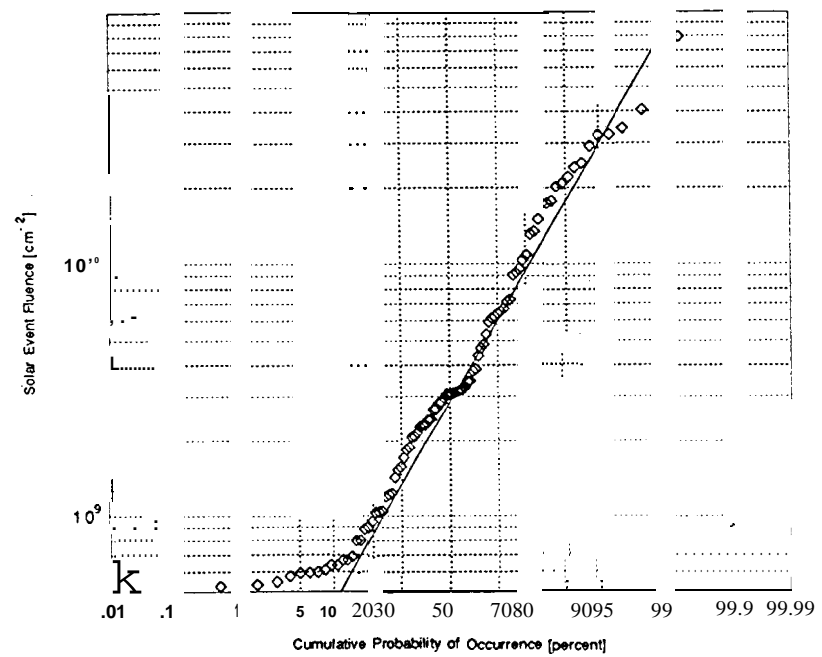
Fig. 5e. Distribution of daily proton fluences for solar active years between 1963 and 1991 for protons of energy >60 MeV.

1001
0









1990
9

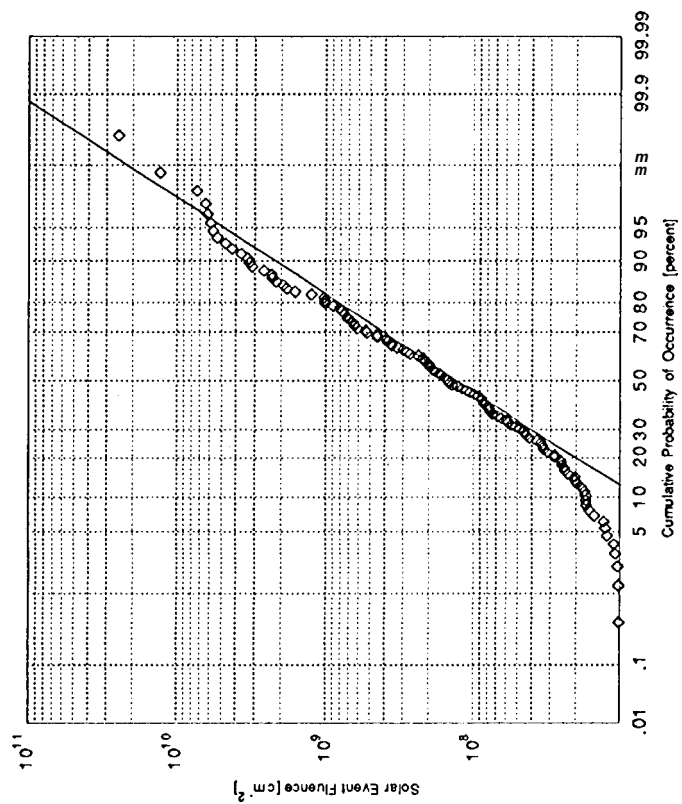


Fig. 2c

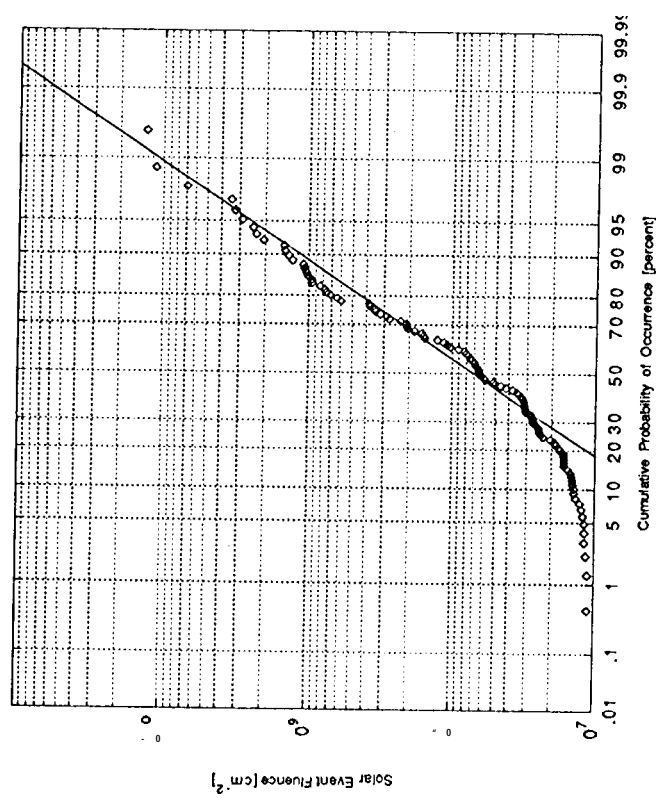
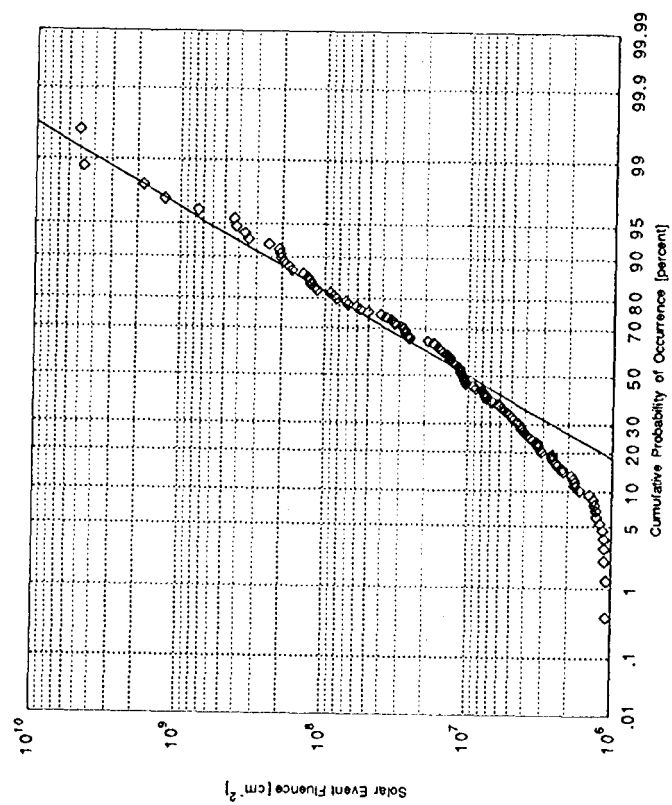


Fig. 2.4



167
0

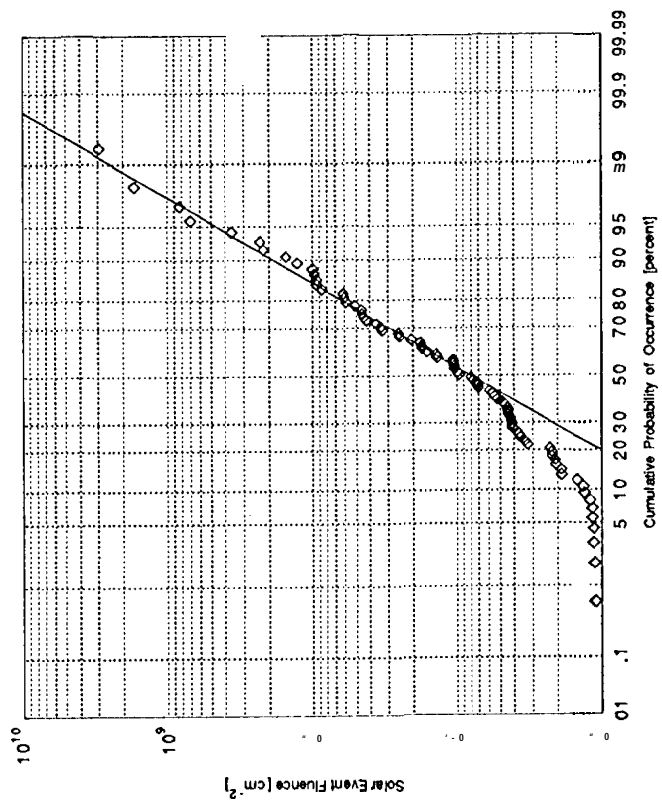
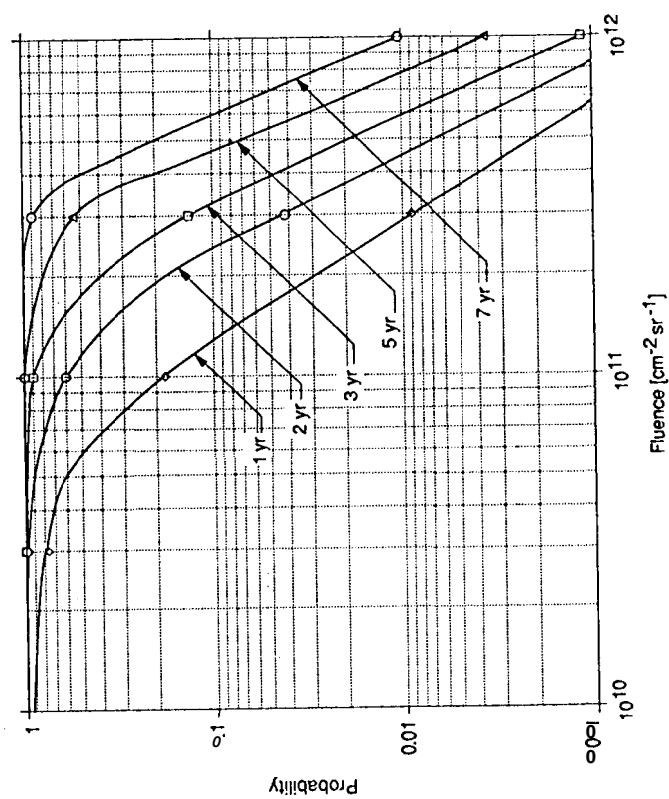
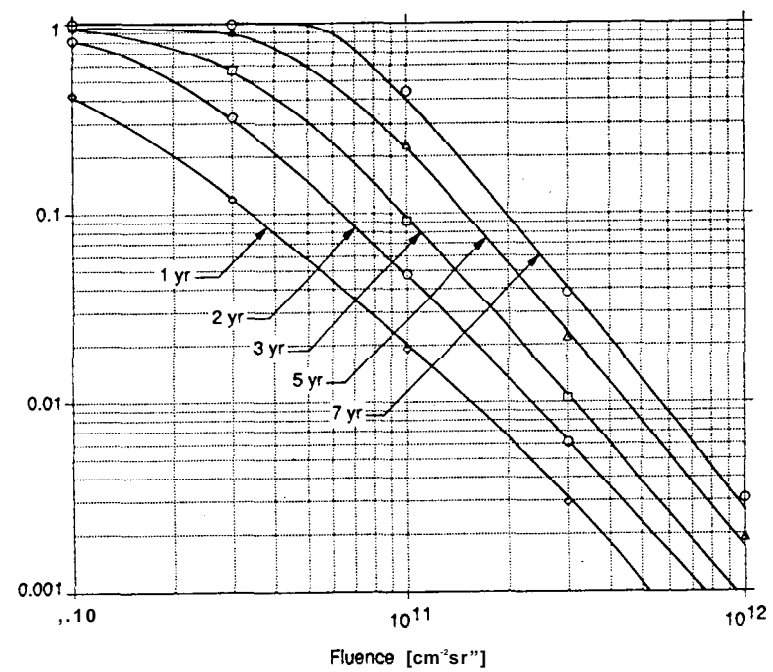
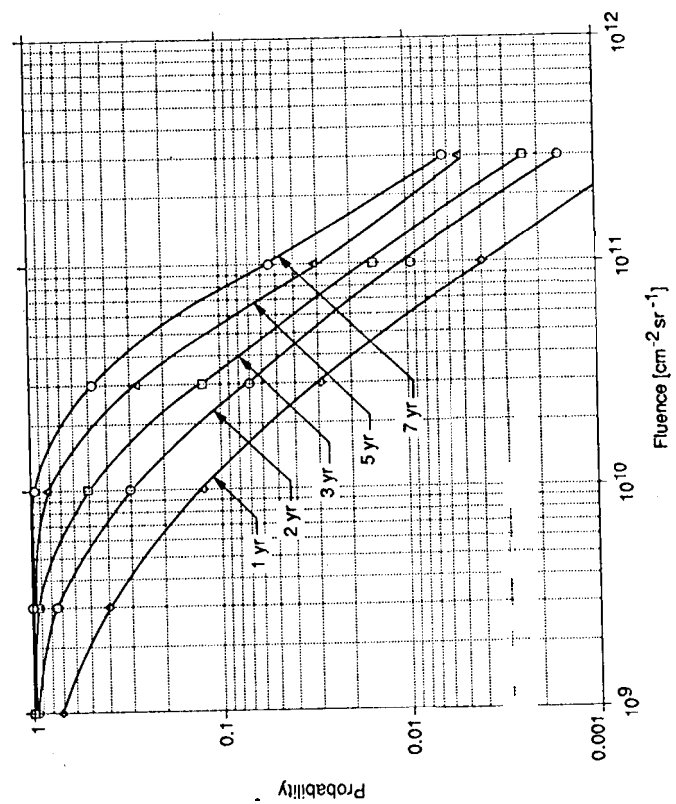


Fig. 40





100 yr
0



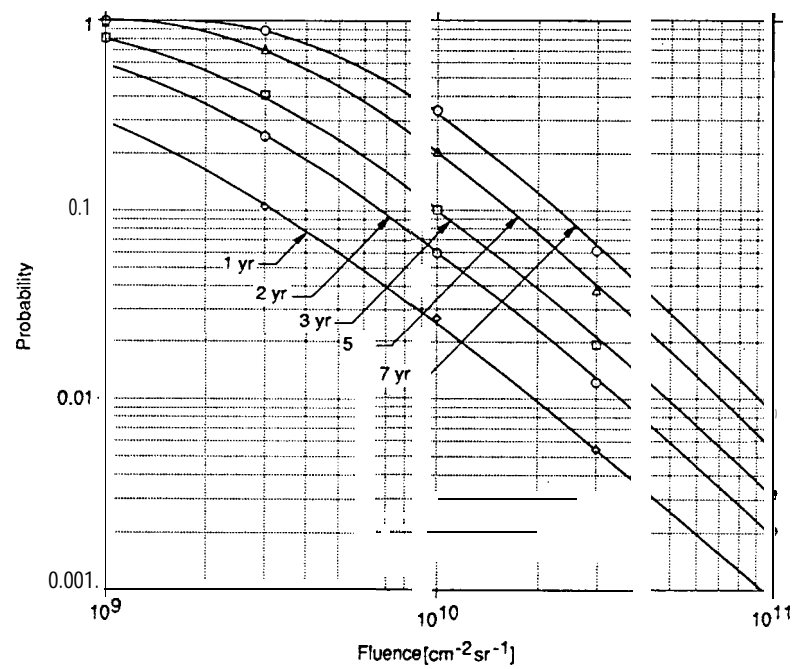
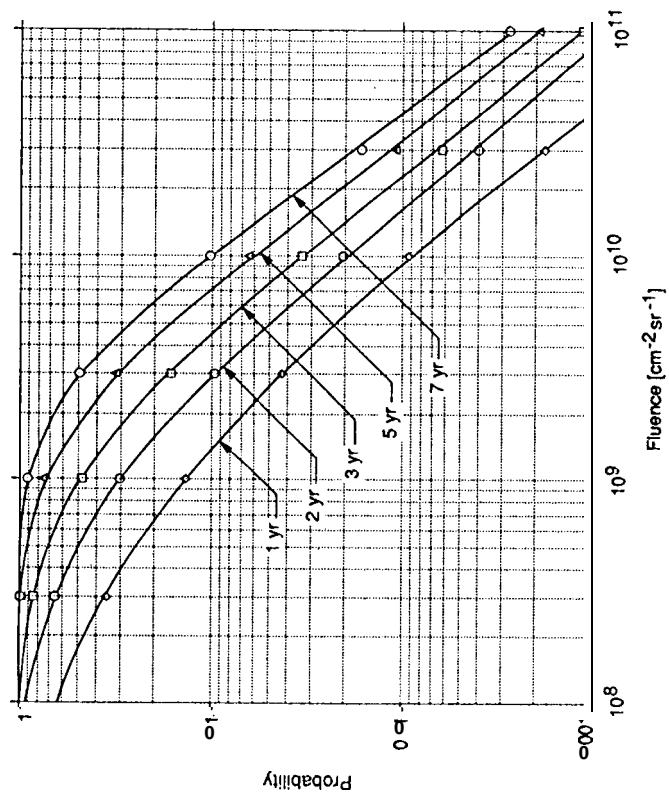


Fig. 4.



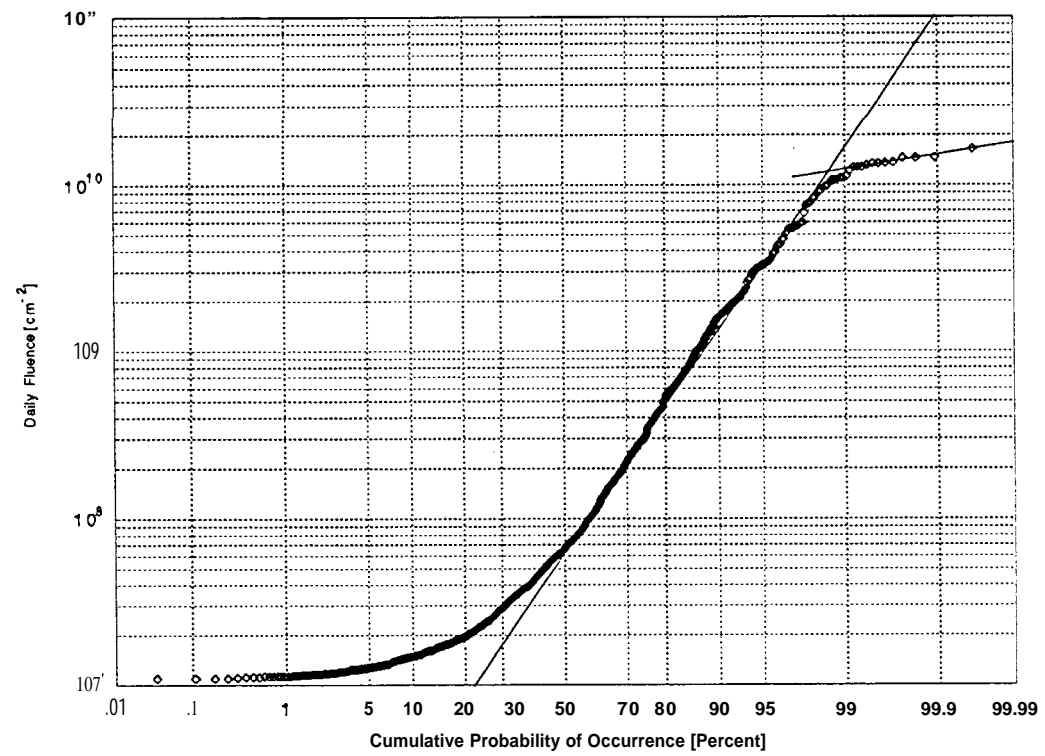
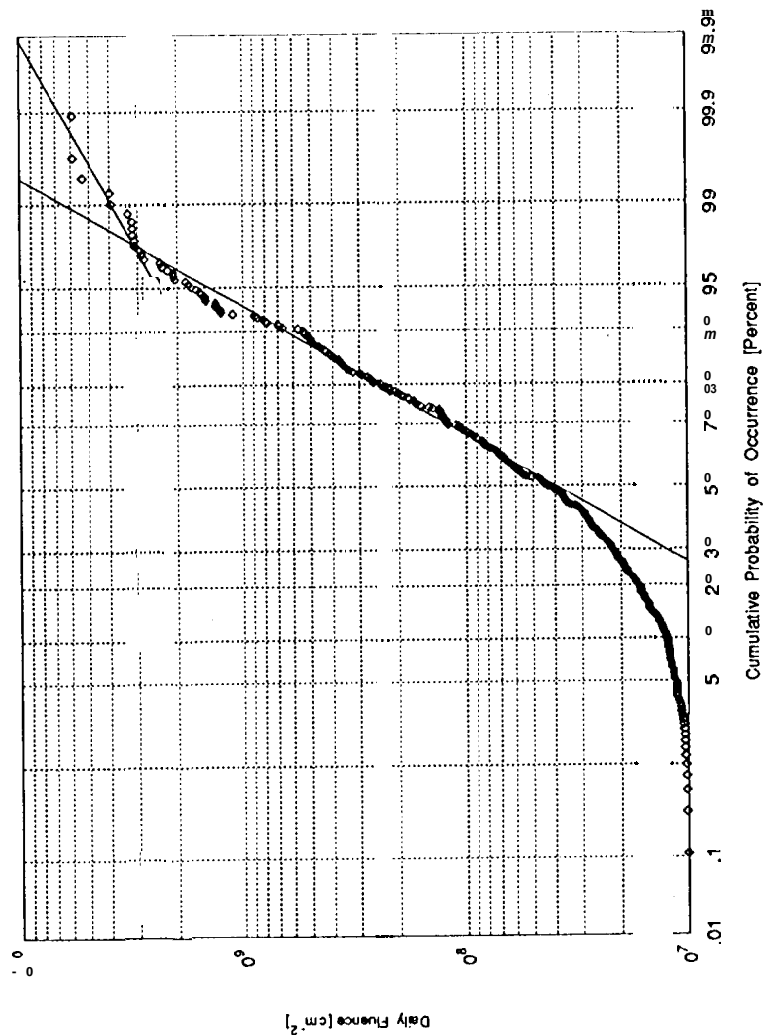


Fig. 500



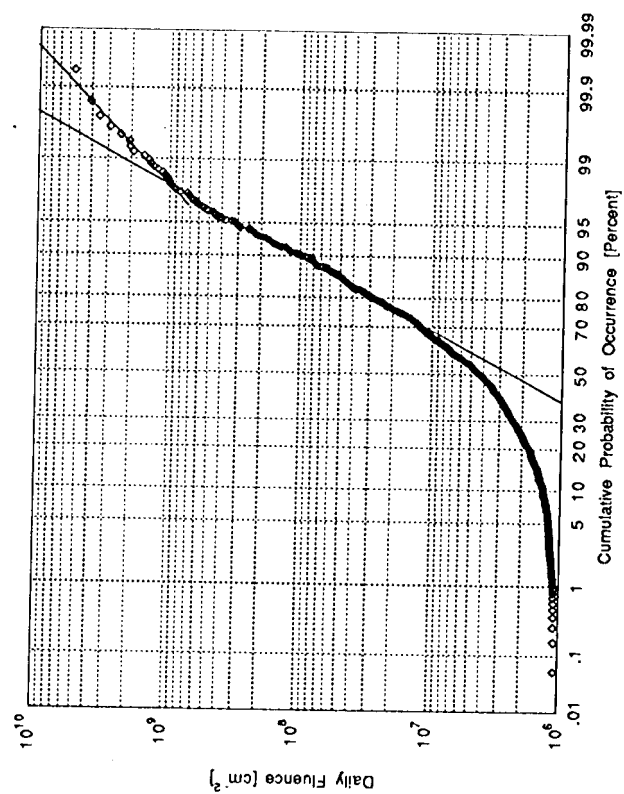
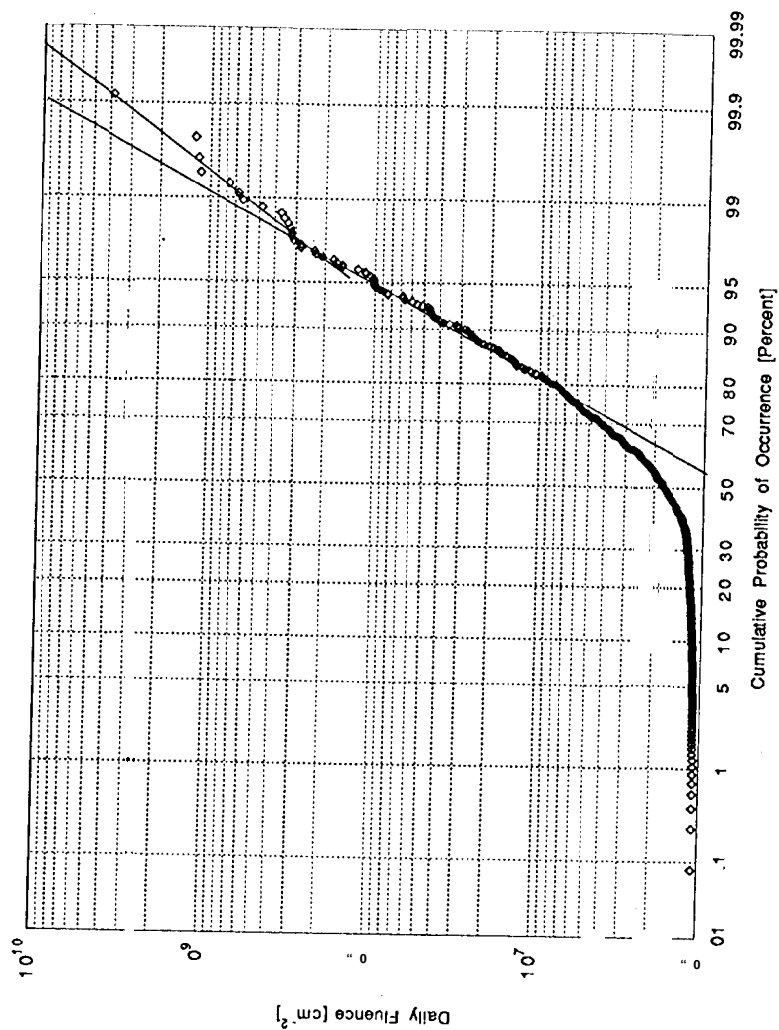


Fig. 5d



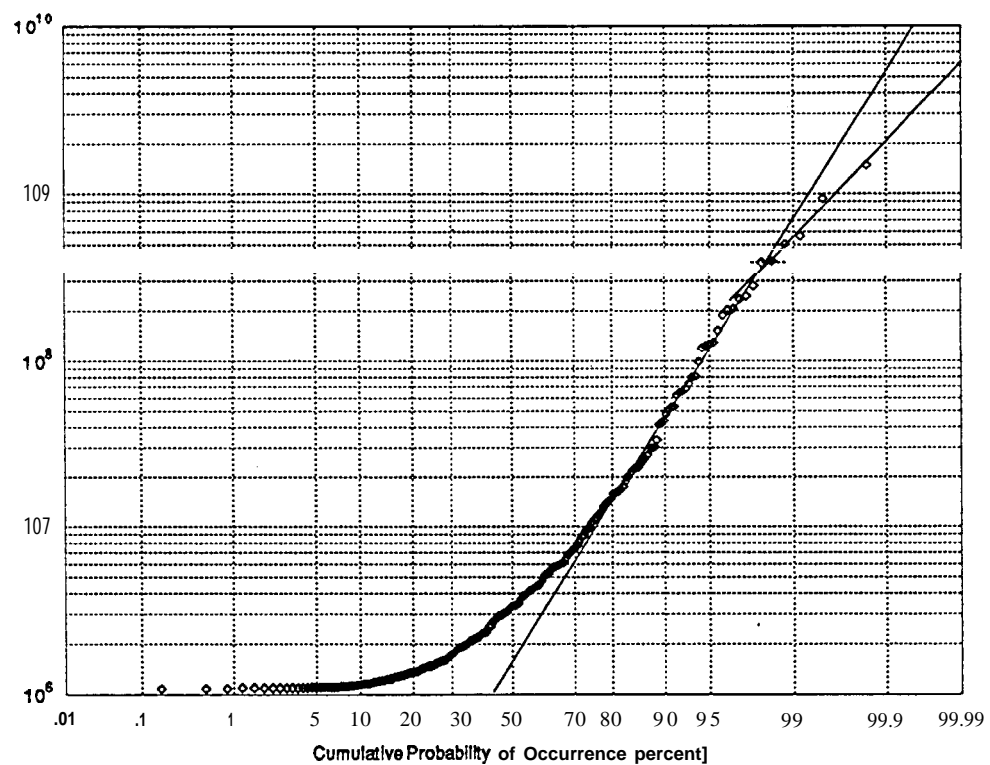


TABLE 1. Ftux Thresholds for Energy Ranges

Energy Range, MeV	Flux Threshold, cm ⁻² sec ⁻¹ sr ⁻¹
>1	10
>4	5
>10	1
>30	1
>60	1

TAB L122. Parameters Used in Monte Carlo Calculation

Parameter	>1 Mev	>4 Mev	>10 Mev	>30 Mev	>60 Mev
Mean, μ	3.0 E9	1.3 E8	7.3 E1	1.0 E7	8.0 E6
Standard deviation of log, σ	0.61	0.96	0.97	1.10	1.07
Range of fluence	>5 E8	>1 E7	>1 E7	>1 E6	>1 E6
Average number/year	8.40	11.5	6.75	7.22	4.73
Number of years	10.6	10.6	16.9	16.9	16.9
Total number of events	89	122	114	122	80

TABLE 3a. Fluence Values for the 10 Largest Events in the Range Where Energy >1 MeV

Year	First Day	Last Day	>1 MeV Fluence
1989	272	314	7.92E+10
1989	225	251	4.05E+10
1978	113	130	3.43E+10
1981	126	147	3.24E+10
1989	66	80	3.23E+10
1981	281	295	2.92E+10
1991	68	102	2.50E+10
1978	44	51	2.40E+10
1982	325	357	2.20E+10
1989	331	340	2.07E+10

Read 7.92E+10 as 7.92.x1010. Values are in 10¹⁰ cm⁻². These data cover day 270 of 1972 through day 126 of 1991.

TABLE 3b. Fluence Values for the 10 Largest Events in the Range Where Energy >4 MeV

Year	First Day	Last Day	>4 MeV Fluence
1989	292	313	24.80E+9
1989	225	249	13.00E+9
1978	112	129	7.31E+9
1978	266	271	6.39E+9
1991	82	90	6.21E+9
1981	281	294	5.87E+9
1989	272	282	5.69E+9
1978	44	49	5.33E+9
1989	331	338	4.69E+9
1981	126	147	4.23E+9

Read 24.8E+9 as 24.8 x 10⁹. Values are in 10¹⁰ cm⁻². These data cover day 270 of 1972 through day 126 of 1991.

TABLE 3c. Fluence Values for the 10 Largest Events in the Range
Where Energy > 10 MeV

Year	First Day	Last Day	>10 MeV Fluence
1989	292	313	13.10E+9
1972	201	233	11.30E+9
1989	225	249	6.89E+9
1989	272	288	3.41E+9
1991	82	98	3.23E+9
1978	266	271	2.88E+9
1978	107	129	2.42E+9
1969	89	113	2.30E+9
1981	281	294	2.06E+9
1971	25	30	1.49E+9

Read 13.1 E+9 as 13.1×10^9 . Values are in 10^{10} cm^{-2} . These data cover day 331 of 1963 through day 126 of 1991.

TABLE 3d. Fluence Values for the 10 Largest Events in the Range
Where Energy >30 MeV

Year	First Day	Last Day	>30 MeV Fluence
1972	173	232	50.20E+8
1989	292	311	47.30E+8
1989	225	244	18.10E+8
1989	272	282	12.90E+8
1991	82	89	7.59E+8
1978	266	269	4.31E+8
1 9 8 1	281	291	4.151X8
1984	116	122	3.60E+8
1971	24	29	3.41E+8
1978	118	123	2.47E+8

Read 50.2E+8 as 50.2×10^8 . Values are in 10^{10} cm^{-2} . These data cover day 331 of 1963 through day 126 of 1991.

TABLE 3e. Fluence Values for the 10 Largest Events in the Range
Where Energy >60 MeV

Year	First Day	Last Day	>60MeV Fluence
1989	292	307	29.60E+8
1972	216	222	16.80E+8
1989	225	243	8.28E+8
1989	272	280	7.01E+8
1991	82	88	3.60E+8
1981	281	291	2.33E+8
1978	266	269	2.20E+8
1978	118	123	1.53E+8
1990	134	134	1.27E+8
1989	334	336	1.00E+8

Read 29.6E+8 as 29.6×10^8 . Values are in 10^{10} cm^{-2} . These data cover day 331 of 1963 through day 126 of 1991.

TABLE 4. Fluence Values for 80% and 95% Confidence Levels for a 2-Year Exposure for JPL 85 and 91 Models

Energy Range, MeV	Confidence Level	JPL 85	JPL 91
>1	80%	...	1.9 E11
>1	95%	...	2.9 E11
>4	80%	...	4.0 E10
>4	95%	...	1.0 E11
>10	80%	2.5 E10	1.3 E10
>10	95%	7.73310	3.8 E10
>30	80%	5.0 E9	3.6 E9
>30	95%	15 E9	11.0 E9
>60	80%	...	1.5 E9
>60	95%	...	5.0 E9

TABLE 5a. Fluence Values for the 10 Highest Fluence Days in the Range Where Energy >1 MeV

Year	Day	>1 MeV Fluence
1983	35	1.65E+10
1978	45	1.47E+10
1989	293	1.46E+10
1978	120	1.37E+10
1979	158	1.36E+10
1989	226	1.35E+10
1978	121	1.32E+10
1991	83	1.29E+10
1989	72	1.28E+10
1981	287	1.23E+10

Read 1.65 E+10 as 1.65×10^{10} . Values are in 10^{10} cm^{-2} . These data cover day 270 of 1972 through day 126 of 1991.

TABLE 5b. Fluence Values for the 10 Highest Fluence Days in the Range Where Energy >4 MeV

Year	Day	>4 MeV Fluence
1989	296	5.85E+9
1989	225	5.83E+9
1989	293	5.29E+9
1978	45	3.97E+9
1978	267	3.91E+9
1989	273	3.29E+9
1990	83	3.15E+9
1989	335	3.14E+9
1989	297	3.13E+9
1988	77	3.07E+9

Read 5.85E+9 as 5.85×10^9 . Values are in 10^{10} cm^{-2} . These data cover day 270 of 1972 through day 126 of 1991.

TABLE 5c. Fluence Values for the 10 Highest Fluence Days in the Range Where Energy >10 MeV

Year	Day	>10 MeV Fluence
1972	217	5.45E+9
1989	225	4.09E+9
1989	296	3.51E+9
1989	293	2.91E+9
1972	218	2.41E+9
1989	273	2.06E+9
1978	267	2.03E+9
1972	221	1.93E+9
1989	298	1.58E+9
1989	295	1.46E+9

Read 5.45E+9 as 5.45×10^9 . Values are in 10^{10} cm^{-2} . These data cover day 331 of 1963 through day 126 of 1991.

TABLE 5d. Fluence Values for the 10 Highest Fluence Days in the Range Where Energy >30 MeV

Year	Day	>30 MeV Fluence
1972	217	38.50E+8
1989	293	12.40E+8
1989	225	11.80E+8
1989	296	11.50E+8
1989	273	7.65E+8
1989	295	6.74E+8
1972	218	6.35E+8
1989	298	4.81E+8
1989	2 9 7	3.70E+8
1989	294	3.55E+8

Read 38.50E+8 as 38.50×10^8 . Values are in 10^{10} cm^{-2} . These data cover day 331 of 1963 through day 126 of 1991.

TABLE 5e. Fluence Values for the 10 Highest Fluence Days in the Range Where Energy >60 MeV

Year	Day	>60 MeV Fluence
1972	217	14.90E+8
1989	293	9.42E+8
1989	296	5.64E+8
1989	225	5.05E+8
1989	295	4.07E+8
1989	273	3.97E+8
1989	298	2.81E+8
1989	292	2.44E+8
1989	294	2.34E+8
1989	272	2.06E+8

Read 14.90E+8 as 14.90×10^8 . Values are in 10^{10} cm^{-2} . These data cover day 331 of 1963 through day 126 of 1991.

7514 Energetic Particles

INTERPLANETARY PROTON FLUENCE MODEL: JPL 1991

J. Feynman, G. Spitale, J. Wang (Jet Propulsion Laboratory, California Institute of Technology, Pasadena, California 91109)

S. Gabriel

We describe an updated predictive engineering model for the interplanetary fluence of protons with energies >1 , >4 , >10 , >30 , and >60 MeV. This has been the first opportunity to derive a model from a data set that has been collected in space over a long enough period of time to produce a valid sample of solar proton events. The model provides a quantitative basis for estimating the exposures to solar protons of spacecraft during missions of varying length and of surfaces and atmospheres of solar system objects. It is derived from the set of data collected by the IMP and OGO spacecraft between 1963 and 1991. The >10 and >30 MeV data sets cover the period from 1963 to day 126 of 1991. The >1 , >4 , and >60 MeV data sets were collected between 1973 and 1991. Both data sets contain several major proton events (>10 -MeV fluences exceeding 3 or 4×10^9 protons/cm²) comparable to the 1972 event. The method of statistical analysis used in producing the model of the proton environment is the same as that used for earlier models. For the cases of the >10 and >30 MeV particles, the fluences are somewhat 10% lower than in our earlier model (JPL 85). No >1 , >4 , and >60 MeV proton fluence models have been published in the literature previously. We present our results in a convenient graphical form which may be used to calculate the 1 AU fluence expected at a given confidence level as a function of the length of the exposure. A method of extending this estimate to other heliocentric distances is described. (Energetic Particles)